8208 *Inorg. Chem.* **2010**, *49*, 8208–8221
DOI: 10.1021/ic902595c

Inorganic Chemistry
Article

Synthesis and Iron Sequestration Equilibria of Novel Exocyclic 3-Hydroxy-2-pyridinone Donor Group Siderophore Mimics

James M. Harrington,[†] Sumathi Chittamuru,[‡] Suraj Dhungana,[†] Hollie K. Jacobs,[‡] Aravamudan S. Gopalan,*[,‡] and Alvin L. Crumbliss*[,†]

[†]*Department of Chemistry, Duke University, Durham, North Carolina 27708-0346, and* [‡]*Department of Chemistry and Biochemistry, New Mexico State University, Las Cruces, New Mexico 88003-8001*

Received December 31, 2009

The synthesis of a novel class of exocyclic bis- and tris-3,2-hydroxypyridinone (HOPO) chelators built on N^2 and N^3 aza-macrocyclic scaffolds and the thermodynamic solution characterization of their complexes with Fe(III) are described. The chelators for this study were prepared by reaction of either piperazine or *N*,*N*′,*N*″-1,4,7-triazacyclononane with a novel electrophilic HOPO iminium salt in good yields. Subsequent removal of the benzyl protecting groups using HBr/acetic acid gave bis-HOPO chelators $N^2(etLH)_2$ and $N^2(prLH)_2$, and tris-HOPO chelator $N^3(etLH)_3$ in excellent yields. Solution thermodynamic characterization of their complexes with Fe(III) was accomplished using spectrophotometric, potentiometric, and electrospray ionization-mass spectrometry (ESI-MS) methods. The pK_a's of $N^2(etLH)_2$, $N^2(prLH)_2$, and $N^3(etLH)_3$, were determined spectrophotometrically and potentiometrically. The Fe(III) complex stability constants for the tetradentate $N^2(etLH)_2$ and $N^2(prLH)_2$, and hexadentate $N^3(etLH)_3$, were measured by spectrophotometric and potentiometric titration, and by competition with ethylenediaminetetraacetic acid (EDTA). $N^3(etLH)_3$ forms a 1:1 complex with Fe(III) with log $\beta_{110} = 27.34 \pm 0.04$. $N^2(prLH)_2$ forms a 3:2 L:Fe complex with Fe(III) where log $\beta_{230} = 60.46 \pm 0.04$ and log $\beta_{110} = 20.39 \pm 0.02$. While $N^2(etLH)_2$ also forms a 3:2 L:Fe complex with Fe(III), solubility problems precluded determining log β_{230}; log β_{110} was found to be 20.45 ± 0.04. The pFe values of 26.5 for $N^3(etLH)_3$ and 24.78 for $N^2(prLH)_2$ are comparable to other siderophore molecules used in the treatment of iron overload, suggesting that these hydroxypyridinone ligands may be useful in the development of new chelation therapy agents.

Introduction

Virtually all forms of life depend on iron to carry out processes necessary for their survival. However, in a pH 7 environment, iron is extremely insoluble ($[Fe^{3+}]_{aq} = \sim 10^{-10}$ mol dm^{-3}) and is usually found in the form of iron hydroxides or oxides because of hydrolysis.[1,2] To overcome problems of limited availability, micro-organisms have developed methods of safely and effectively extracting iron from the environment through manipulating the inner coordination sphere of the metal ion to form soluble complexes.[3] Bacteria and fungi produce small-molecule iron-specific chelators, siderophores, to aid in the uptake of iron by sequestering the metal ion with high stability and specificity (log $\beta > 25$).[4−7]

Excess iron is toxic because it can potentially react with the various oxidation states of oxygen in a biological system to form reactive oxygen species through redox cycling, damaging the organism and even causing death.[8] An effective method of treating iron overload disease and hemochromatosis involves the use of iron chelation therapy. There are currently two U.S. FDA-approved therapeutic agents for iron-overload, Desferal (desferrioxamine B mesylate, DFB), and Exjade (deferasirox), (see below).[9−11] However, these agents are both problematic. Desferal suffers from low

*To whom correspondence should be addressed. E-mail: alc@chem.duke.edu (A.L.C.), agopalan@nmsu.edu (A.S.G.). Fax: (919) 660-1605 (A.L.C.); (575) 646-2649 (A.S.G.).

(1) Boukhalfa, H.; Crumbliss, A. L. *Biometals* **2002**, *15*, 325–339.
(2) Kragter, J. *Atlas of Metal-Ligand Equilibria in Aqueous Solution*; Halstead Press: New York, 1978.
(3) Crichton, R. R. *Inorganic Biochemistry of Iron Metabolism*, 2nd ed.; Ellis Horwood, Ltd.: Chichester, U.K., 2001.
(4) Albrecht-Gary, A. M.; Crumbliss, A. L. In *Metal Ions in Biological Systems*; Sigel, A., Sigel, H., Ed.; Marcel Dekker: New York, 1998; Vol. *35*, pp 239−327.
(5) Crumbliss, A. L.; Harrington, J. M. In *Advances in Inorganic Chemistry*; van Eldik, R., Hubbard, C. D., Eds.; Academic Press: Orlando, FL, 2009; Vol. *61*, pp 179−250.
(6) Raymond, K. N.; Dertz, E. A. In *Iron Transport in Bacteria*; Crosa, J. H., Rey, A. R., Payne, S. M., Eds.; ASM Press: Washington, D.C., 2004; pp 3−17.
(7) Harrington, J. M.; Crumbliss, A. L. *Biometals* **2009**, *22*, 679–689.
(8) Haber, F.; Weiss, J. *Proc. Royal Soc. London, Ser. A* **1934**, *147*, 332–351.
(9) Jacobs, A. J. In *Development of Iron Chelators for Clinical Use*; Martell, A. E., Anderson, W. F., Badman, D. B., Eds.; Elsevier/North Holland: New York, 1981; pp 29−46.
(10) Lattmann, R.; Acklin, P.; U.S. Patent No. US 6,465,504 B1 (October 15, 2002).
(11) Nick, H. *Curr. Opin. Chem. Biol.* **2007**, *11*, 419–423.

 Published on Web 08/17/2010

bioavailability, a short half-life in serum, and a treatment regime that includes daily intravenous transfusions, which is a long, painful, and expensive procedure leading to low patient compliance. Exjade is perhaps a better choice, because of its increased bioavailability and the ability to administer the drug orally. However, the molecule lacks specificity for iron, which may result in undesirable side effects because of sequestration of other

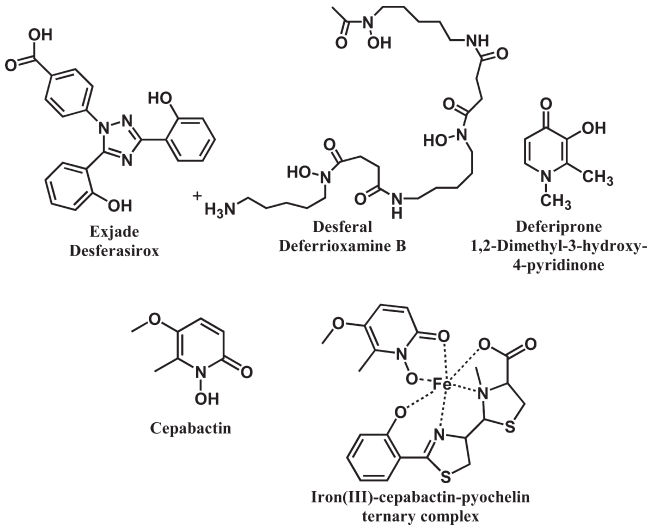

metal ions. Thus, it is desirable to develop new synthetic siderophores to treat iron overload diseases to find a chelator with high bioavailability and iron specificity.

One high affinity iron(III) binding moiety that is rarely observed in nature is the hydroxypyridinone (HOPO) donor group. The only observed instance of a natural HOPO siderophore is cepabactin, a 1-hydroxy-2-pyridinone bidentate siderophore produced by *Burkholderia cepacia* (above).[12] Cepabactin is one of a number of siderophores produced by the bacteria, and often forms a mixed complex with pyochelin (above) that is less stable than the tris-cepabactin-Fe(III) complex, but more stable than the bis-pyochelin-Fe(III) complex.[13]

Hydroxypyridinones are similar to catechol donor groups in their affinity for Fe(III) because of the similar electronic configurations of the two moieties (eqs 1 and 2).[14−16] However, their

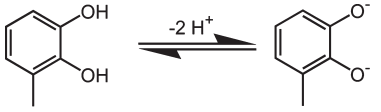

(1)

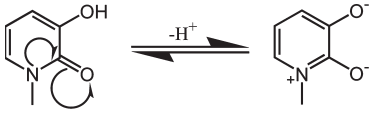

(2)

different number of donor moiety ionizable protons (one for HOPO and two for catechol) results in less H^+ competition and more effective Fe(III) chelation by HOPO donor groups, as reflected in the pFe values for catechol (15.1) and 3,2-HOPO (16.26).[17−20] The charge difference in the donor moieties of catechol and HOPO also affect the equilibrium constants for complexation. This is demonstrated by comparing the *stepwise* formation constants for the iron-catechol complex with those of the 3,2-HOPO complex.[18,19] The K_1 for $FeL(OH_2)_4^{n+}$ formation (where K represents the proton independent stepwise formation constant) is larger for L = catechol than for 3,2-HOPO, at least partially because of the greater electrostatic force of attraction between the +3 iron and the catechol dianion. However, apparently the higher negative charge for catechol also has a destabilizing effect because of charge repulsion in the higher order complexes. Normally, the stepwise equilibrium constants decrease in the order $K_1 > K_2 > K_3$ for statistical reasons. However, the observed decrease is greater than expected on statistical grounds for catechol ($K_1 = 20.4$, $K_2 = 15.5$, $\Delta_{1-2} = 4.9$, $K_3 = 9.4$, $\Delta_{2-3} = 6.1$) than for 3,2-HOPO ($K_1 = 11.48$, $K_2 = 9.77$, $\Delta_{1-2} = 1.71$, $K_3 = 8.01$, $\Delta_{2-3} = 1.76$) because of increased charge repulsion.[19,21]

There are ostensibly two types of linkages that have been used for the connection of multiple 3,2-HOPO donor groups in the design of polydentate hydroxypyridinone siderophore mimics. A key distinction is that in the *HOPO* system shown below, the 3,2-HOPO ligand is attached to the scaffold through the pyridinone nitrogen, while for the *retroHOPO* system, an amide linkage on the 3,2-HOPO ring is used for connection with the backbone. The orientation of the donor

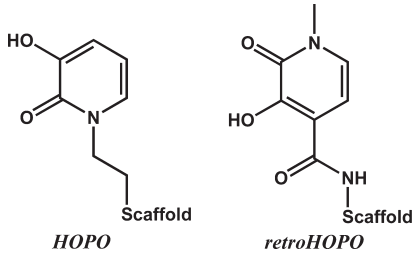

groups in the siderophore mimics differ in these two systems, and this difference plays a role in metal complexation equilibria. The presence of an amide functional group conjugated to the pyridyl ring in the *retroHOPO* system has an effect on the acidity of the hydroxypyridinone moiety. Comparison of the hydroxypyridinone protonation constants for TRENHOPO and TRISPYR (Figure 1) provides a demonstration of this effect.[15,22] The average pK_a of the hydroxypyridinone donor groups of TRISPYR, which features the *HOPO* type donor group is 9.50, while the average pK_a of the *retroHOPO* donor groups of TRENHOPO is 6.99. This greater acidity in the *retroHOPO* donor group is possibly

(12) Thomas, M. S. *Biometals* **2007**, *20*, 431–452.
(13) Klumpp, C.; Burger, A.; Mislin, G. L.; Abdallah, M. A. *Bioorg. Med. Chem. Lett.* **2005**, *15*, 1721–1724.
(14) Scarrow, R. C.; Riley, P. E.; Abu-Dari, K.; White, D. L.; Raymond, K. N. *Inorg. Chem.* **1985**, *24*, 954–967.
(15) Xu, J.; O'Sullivan, B.; Raymond, K. N. *Inorg. Chem.* **2002**, *41*, 6731–6742.
(16) Abergel, R. J.; Raymond, K. N. *Inorg. Chem.* **2006**, *45*, 3622–3631.
(17) L'Heureux, G.; Martell, A. E. *J. Inorg. Nucl. Chem.* **1966**, *28*, 481–491.
(18) Martell, A. E.; Smith, R. M. *Critical Stability Constant Database*; National Institute of Science and Technology (NIST): Gaithersburg, MD, 2003.
(19) Clarke, E. T.; Martell, A. E. *Inorg. Chim. Acta* **1992**, *196*, 185–194.
(20) Motekaitis, R. J.; Martell, A. E. *Inorg. Chim. Acta* **1991**, *183*, 71.
(21) Avdeef, A.; Sofen, S. R.; Bregante, T. L.; Raymond, K. N. *J. Am. Chem. Soc.* **1978**, *100*, 5362–5370.
(22) Sun, Y.; Motekaitis, R. J.; Martell, A. E. *Inorg. Chim. Acta* **1998**, *281*, 60–63.

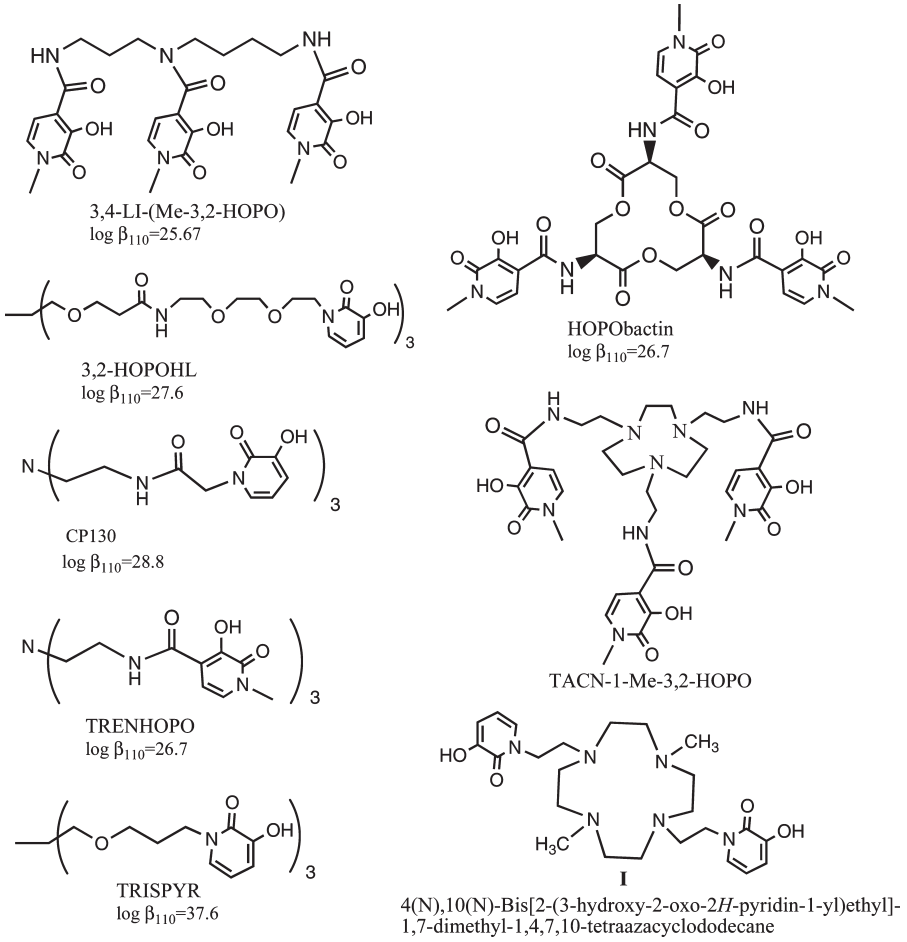

Figure 1. Representative synthetic 3,2-hydroxypyridinone siderophore mimics. Stability constants taken from refs 16, 22, 40, 60, and 61.

due to inductive effects arising from the proximity of the amide connector to the pyridyl ring.

The drug deferiprone, or 1,2-dimethyl-3-hydroxy-4-pyridinone (above), is a bidentate 3,4-HOPO chelator that has been approved for use in chelation therapy treatments in Europe.[23] However, questions have been raised with respect to the toxicity of this drug, related to binding efficiency and its possible role in the development of diseases, including hepatic fibrosis and a variety of other disorders.[24−26] There are also questions related to the redox chemistry of its iron complexes.[27] The development of chelation therapy agents requires that the metal free chelator have high bioavailability to allow ease of uptake, but that the metal complex formed have low bioavailability, to aid in removal of the metal from the system.

The low bioavailability and high stability of previously characterized Fe(III)-HOPO complexes suggests that the development of synthetic siderophores with hydroxypyridinone donors may be a viable route for the development of new treatments for iron overload disease. Preliminary studies on the use of HOPO siderophores as a treatment for iron overload disease have shown promising results with regard to iron binding ability and lack of bioavailability of the iron(III) complexes in mammalian systems.[28,29] In addition to iron overload chelation therapy agents, HOPO chelators and other iron chelators have other potential medical applications. These include the development of novel antibacterial agents, and cancer prevention and treatment agents.[30] Hydroxypyridinone chelators also form strong complexes with other hard metal ions leading to additional potential applications. They have been examined for their ability to achieve in vivo clearance of Pu(IV) ions, as potential extraction agents for Pu(IV), and have been attached to calix[4]-arenes to yield useful Th(IV) extractants.[31,32] Gadolinium HOPO chelate complexes have been prepared and shown to have potential as contrast agents in magnetic resonance imaging (MRI).[33−36] As chelators of Ga-67 and In-111,

(23) Capellini, M. D.; Pattoneri, P. *Annu. Rev. Med.* **2009**, *60*, 25–38.
(24) Kontoghiorghes, G. J. *Expert Opin. Drug Saf.* **2007**, *6*, 235–239.
(25) Olivieri, N. F.; Brittenham, G. M.; McLaren, C. E.; Templeton, D. M.; Cameron, R. G.; McClelland, R. A.; Burt, A. D.; Fleming, K. A. *N. Eng. J. Med.* **1998**, *339*, 417–423.
(26) Wu, S. F.; Peng, C. T.; Wu, K. H.; Tsai, C. H. *Hemoglobin* **2006**, *30*, 215–218.
(27) El-Jammal, A.; Templeton, D. M. *Inorg. Chim. Acta* **1996**, *245*, 199–207.
(28) Hider, R. C.; Kontoghiorghes, G. J.; Silver, J.; Brit. U.K. Patent Appl.: Great Britain, 1984; p 17.
(29) Hider, R. C.; Kontoghiorghes, G. J.; Silver, J.; Stockton, M. A.; Brit. U.K. Patent Appl.: Great Britain, 1984; p 19.
(30) Weinberg, E. D. *Adv. Appl. Microbiol.* **2003**, *52*, 187–208.
(31) Veeck, A. C.; White, D. J.; Whisenhunt, D. W., Jr.; Xu, J.; Gorden, A. E. V.; Romanovski, V.; Hoffman, D. C.; Raymond, K. N. *Solvent Extr. Ion Exch.* **2004**, *22*, 1037–1068.
(32) Lambert, T. N.; Dasaradhi, L.; Huber, V. J.; Gopalan, A. S. *J. Org. Chem.* **1999**, *64*, 6097–6101.
(33) Werner, E. J.; Datta, A.; Jocher, C. J.; Raymond, K. N. *Angew. Chem.* **2008**, *47*, 85688580.
(34) Pierre, V. C.; Botta, M.; Aime, S.; Raymond, K. N. *J. Am. Chem. Soc.* **2006**, *128*, 5344–5345.

HOPO ligands are potentially useful as radiopharmaceutical imaging agents.[37,38] The numerous potential applications of HOPO chelators highlight the need to develop methods for their synthesis that are flexible and enable their attachment to a variety of molecular platforms.

The most common method for the preparation of 3,2-HOPO chelators involves the coupling of an amine with an activated carboxylic acid linker attached to the pyridinone ring system.[39] In the case of polyHOPO derivatives, this method results in multiple amide bonds which can limit both organic and aqueous solubility. Several examples of amide linked tris-HOPO siderophores are shown in Figure 1. TRENHOPO, 3,2-HOPOHL, and CP130, all have a similar tripodal design with the three chelating arms attached to a central atom using an amide-linked spacer group. The iron(III) affinity for these siderophores range from pFe = 26.8 to 32.23.[22,40] Compared to the amide linked tripodal chelators, the linear tris-HOPO chelator, 3,4-LI-(Me-3,2-HOPO), exhibits a slightly lower complex stability, pFe = 25.5.[16] The tripodal chelator, TRISPYR, which does not have amide linkages, was prepared by direct alkylation of the backbone amine resulting in low yields of the desired product.[22] The very high iron(III) affinity of TRISPYR, pFe = 32.23, was attributed to the flexibility in the ether linkages to the three hydroxypyridinones.[22] While the presence of amide linking groups may contribute to decreased ligand solubility and increased susceptibility to enzymatic hydrolysis, their presence can also contribute to complex stability through the formation of hydrogen bonding networks, which may act to preorganize the ligand binding site. Additionally, in natural siderophores and synthetic mimics, the amide moieties such as in catecholamide donor groups have been proposed to play a role because of binding mode shifts over a range of pH values.[41−43]

Very few poly-HOPO chelators built on a cyclic backbone have been synthesized. HOPObactin, (Figure 1, pFe = 26.8) is a 3,2-hydroxypyridinone analogue of the catechol siderophore enterobactin and is built on a trilactone core.[40] This ligand exhibits low solubility in water, and the trilactone core is susceptible to hydrolysis above pH 8, as well as below pH 6. By comparing the binding constants of HOPObactin with the tripodal tris HOPO ligands, it is clear that the trilactone core does not impart additional stabilization for the anchored HOPO binding moieties. The trisHOPO chelator, TACN-1-Me-3,2-HOPO (Figure 1), is built on an azamacrocyclic platform with the three 3,2-HOPO chelating groups attached by amide bonds.[36] This chelator exhibits better solubility

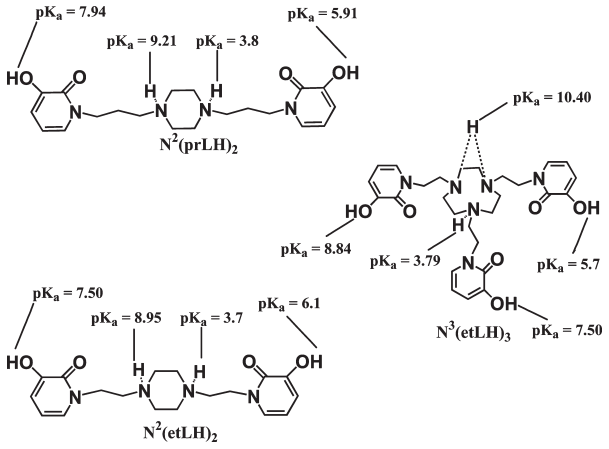

Figure 2. Structures and measured pK_a's of the synthetic exocyclic 3-hydroxy-2-pyridinone donor group siderophores in this study: N^2-(etLH)$_2$, N^2(prLH)$_2$, and N^3(etLH)$_3$. pK_a values listed are from Table 1. Distinction between assignments for pK_{a1} and pK_{a4}, and pK_{a2} and pK_{a3} for N^2(etLH)$_2$ and N^2(prLH)$_2$ are arbitrary. Distinction between assignments for pK_{a2}, pK_{a3}, and pK_{a4} for N^3(etLH)$_3$ are arbitrary.

than HOPObactin, and its Gd(III) complex has been examined as a magnetic resonance contrast agent; however, its iron(III) binding properties have not been evaluated. The diHOPO cyclen chelator, **I** (Figure 1), was prepared, and its Zn(II) and Cu(II) binding properties were evaluated.[44] Unfortunately, the iron(III) binding properties were not reported.

Previously, the synthesis of N^2(prLH)$_2$ (Figure 2) was reported using methodology developed in the Gopalan laboratory for the convenient attachment of 3,2-HOPO groups without concomitant formation of an amide bond.[45] It was thought that the azamacrocyclic platform might provide an ideal backbone on which to anchor 3,2-HOPO chelating units. Unlike the trilactone core of enterobactin, the azamacrocyclic backbone is hydrolytically stable over a range of solution pH values, including the physiologically relevant 5−7.4 pH range. Further, the amine groups in the backbone enhance water solubility.

Here we report the synthesis of a new class of bis- and tris-exocyclic synthetic 3,2-HOPO siderophores built on an N^2 and N^3 azamacrocycle platform (Figure 2). The protonation equilibria of these three siderophores were elucidated through potentiometric and spectrophotometric titrations, and the stability of their complexes with Fe(III) was determined through spectrophotometric titration and competition reactions with ethylenediaminetetraacetic acid (EDTA). Evaluation of the iron binding properties of such compounds provides valuable information in the design of iron chelators with desirable therapeutic properties.

Experimental Section

Materials. All solutions were prepared in deionized water. Solid NaCl (>99%, Fisher Chemicals) was used to prepare the background electrolyte solution. Standardized 1 N NaOH solution (Fisher Chemicals) was used to prepare a 0.10 mol

(35) Thompson, M. K.; Misselwitz, B.; Tso, L. S.; Doble, D. M. J.; Schmitt-Willich, H.; Raymond, K. N. *J. Med. Chem.* **2005**, *48*, 3874–3877.
(36) Werner, E. J.; Avedano, S.; Botta, M.; Hay, B. P.; Moore, E. G.; Aime, S.; Raymond, K. N. *J. Am. Chem. Soc.* **2007**, *129*, 1870–1871.
(37) Reichert, D. E.; Lewis, J. S.; Anderson, C. J. *Coord. Chem. Rev.* **1999**, *184*, 3–66.
(38) Miao, Y.; Hylarides, M.; Fisher, D. R.; Shelton, T.; Moore, H.; Wester, D. W.; Fritzberg, A. R.; Winkelmann, C. T.; Hoffman, T.; Quinn, T. P. *Clin. Cancer Res.* **2005**, *11*, 5616–5621.
(39) Rai, B. L.; Khodr, H.; Hider, R. C. *Tetrahedron* **1999**, *55*, 1129–1142.
(40) Meyer, M.; Telford, J. R.; Cohen, S. M.; White, D. J.; Xu, J.; Raymond, K. N. *J. Am. Chem. Soc.* **1997**, *119*, 10093–10103.
(41) Abergel, R. J.; Warner, J. A.; Shuh, D. K.; Raymond, K. N. *J. Am. Chem. Soc.* **2006**, *128*, 8920–8931.
(42) Stack, T. D. P.; Karpishin, T. B.; Raymond, K. N. *J. Am. Chem. Soc.* **1992**, *114*, 1512–1514.
(43) Raymond, K. N.; Dertz, E. A.; Kim, S. S. *Proc. Natl. Acad. Sci. U.S.A.* **2003**, *100*, 3584–3588.
(44) Ambrosi, G.; Dapporto, P.; Formica, M.; Fusi, V.; Giorgi, L.; Guerri, A.; Lucarini, S.; Micheloni, M.; Paoli, P.; Pontellini, R.; Rossi, P.; Zappia, G. *New J. Chem.* **2004**, *28*, 1359–1367.
(45) Lambert, T. N.; Chittamuru, S.; Jacobs, H. K.; Gopalan, A. S. *Tetrahedron Lett.* **2002**, *43*, 7379–7383.

dm^{-3} solution. The base solution was standardized against KHP (Aldrich, 99.95%) to the phenolphthalein end point. Concentrated HCl (Mallinckrodt AR, 37%) was used to prepare a 0.10 mol dm^{-3} solution, which was standardized against a standard NaOH solution to the phenolphthalein end point. Solid anhydrous $FeCl_3$ was obtained from Sigma and used to prepare 0.10 mol dm^{-3} stock solution that was standardized titrimetrically by reduction with $SnCl_2$, followed by titration with $K_2Cr_2O_7$.[46] Competition reactions were performed with a stock solution prepared from solid EDTA (Acros Organics, 99+%). pK_a titrations of each of the HOPO siderophores alone were performed in $NaClO_4$ background electrolyte, while titrations in the presence of iron(III) were performed in NaCl background electrolyte because of low solubility in perchlorate above pH 4. Hydroxypyridinone alcohol **1** and $N^2(prLH)_2$ were prepared by published procedures.[32,45]

Methods. Potentiometric Measurements. Ligand pK_a's were determined by potentiometric and spectrophotometric titrations. All pH measurements were made with an Orion 230 A+ pH/ion meter equipped with an Orion Ross pH electrode filled with 3 mol dm^{-3} NaCl solution. The electrode was calibrated by titration of standardized 0.10 mol dm^{-3} HCl with standardized 0.10 mol dm^{-3} NaOH, as in the "classical method," and calibration data were analyzed using the computer program, GLEE.[47,48] Ligand solutions were prepared at 6.7×10^{-4} mol dm^{-3} for the $N^2(prLH)_2$ titration and at 4.0×10^{-4} mol dm^{-3} for the $N^3(etLH)_3$ titration in acid and titrated with 0.010 mol dm^{-3} NaOH. Potentiometric data were analyzed with the Microsoft Excel program.[49] Ferric complex solutions were prepared at concentrations of $[Fe^{3+}] = 4.00 \times 10^{-4}$ mol dm^{-3} and $[N^2(prLH)_2] = 6.0 \times 10^{-4}$ mol dm^{-3} for the Fe−$N^2(prLH)_2$ system and $[Fe^{3+}] = 3.98 \times 10^{-4}$ mol dm^{-3} and $[N^3(etLH)_3] = 4.0 \times 10^{-4}$ mol dm^{-3} for the Fe−$N^3(etLH)_3$ system. These solutions were also titrated with 0.010 mol dm^{-3} NaOH, and potentiometric titration data were analyzed with Excel.

Spectrophotometric Titrations. UV−visible spectra were recorded using a Cary-50 spectrophotometer equipped with an external dip probe (Hellma, U.S.A.). For spectrophotometric titrations of the siderophores alone, solutions of 1.0×10^{-5} mol dm^{-3} siderophore were prepared in 0.10 mol dm^{-3} $NaClO_4$ solutions. These solutions were titrated with standardized 0.010 mol dm^{-3} NaOH/0.090 mol dm^{-3} $NaClO_4$ solutions. The pH was measured after each addition, and the UV−visible spectrum was measured in the wavelength region of 200−400 nm. Spectrophotometric data were analyzed by the program SPECFIT to determine the protonation constants of the ligands.[50]

Solutions for use in spectrophotometric titrations were all prepared as described in the Supporting Information. Concentrations of metal and ligand are noted in the captions of the figures showing the titrations. For all of the Fe(III)-siderophore complex titrations, 0.10 mol dm^{-3} NaCl was used as a background electrolyte. The presence of chloride was taken into account in the determination of the stability constants by including the stability constants of the mono-, di-, and trichloroiron(III) complexes in the determinations of the stability constants for the hydroxypyridinone complexes.[18]

Two pH-dependent titrations (acid and base) were performed for each Fe(III)-siderophore system. In the base titration, 0.10 mol dm^{-3} NaOH was used to titrate the Fe(III)-siderophore complex from pH 3.5 to pH 10.9. UV−vis spectra from the titration were analyzed with the programs SPECFIT and HYPERQUAD to determine the protonation constants of the complexes.[50,51] All determined complex stability constants are shown in Table 1.

An acid titration, using 1.0 mol dm^{-3} HCl was conducted for each Fe(III) siderophore system from pH 3.0 to ~pH 0.3. For these titrations, the Microsoft Excel program was used to analyze the spectral shifts because of difficulty of solving for some concentrations in both SPECFIT and HYPERQUAD.[49] Electrode calibration in high-acid conditions was performed assuming Nernstian behavior with a junction potential using the program VLpH.[52]

EDTA Competition Titrations. UV−visible spectra were recorded using a Varian Cary 100 UV−visible spectrophotometer measuring from 350−750 nm. For the $Fe_2(N^2(prL)_2)_3$ system, stock solutions of the Fe(III)-siderophore complex were prepared in 2.0 mL aliquots at $[Fe^{3+}] = 2.47 \times 10^{-4}$ mol dm^{-3} and $[N^2(prLH)_2] = 3.70 \times 10^{-3}$ mol dm^{-3}, and a range of concentrations of EDTA, from 0 to 25 equiv of EDTA relative to Fe(III), were added while monitoring the pH (between 5.5 and 7.1). The competition reaction performed for the $N^2(prLH)_2$ system is shown in eqs 3−4.

$$Fe_2(HN^2(prL)_2)_3^{3+} + 2HEDTA^{3-} + H^+ \leftrightarrows 2Fe(EDTA)^- + 3HN^2(prL)(prLH) \quad (3)$$

$$K_{obs} = \frac{[Fe(EDTA)^-]^2[HN^2(prL)(prLH)]^3}{[Fe_2(HN^2(prL)_2)_3^{3+}][HEDTA^{3-}]^2[H^+]} \quad (4)$$

Solutions of the complexes were allowed to react for 24 h at 25 °C, until the spectra of the solutions were constant, and the pH and UV−visible spectra were measured. Data from the competition titration (Figure 3) were used in conjunction with the published stability constant of the Fe(EDTA) complex to determine the stability constant (Table 1) of the $Fe_2(N^2(prL)_2)_3$ complex using eqs 5−7.

$$2Fe(H_2O)_6^{3+} + 3N^2(prL)_2^{2-} \leftrightarrows Fe_2(N^2(prL)_2)_3 + 6H_2O \quad (5)$$

$$\beta_{230} = \frac{[Fe_2(N^2(prL)_2)_3]}{[Fe(H_2O)_6^{3+}]^2[N^2(prL)_2^{2-}]^3} \quad (6)$$

$$\beta_{230} = \left(\frac{K_{obs}}{(\beta_{110,EDTA})^2}\right)^{-1} \quad (7)$$

The computer program, HYPERQUAD was used to analyze the spectral shifts in the titration of the Fe(III)-$N^2(prLH)_2$ system.[51] The stability constants of the Fe(EDTA) complex and the protonation constants of EDTA were taken from the Critical Stability Constant Database and held constant in the analysis, as were the siderophore protonation constants.[18]

A similar experiment was performed for the $N^3(etLH)_3$ system with the concentrations $[Fe^{3+}] = [N^3(etLH)_3] = 4.0 \times 10^{-4}$ mol dm^{-3} and the EDTA concentration ranging from 0 to 0.01 mol dm^{-3}, and the solution pH ranging from 5.5 to

(46) Vogel, A. I. *A Text-Book of Quantitative Inorganic Analysis*, 3rd ed.; Longmans, Green, and Co Ltd: London, 1961.
(47) Martell, A. E.; Motekaitis, R. J. *Determination and Use of Stability Constants*, 2nd ed.; VCH Publishers: New York, 1992.
(48) Gans, P.; O'Sullivan, B. *Talanta* **2000**, *51*, 33–37.
(49) Billo, E. J. *EXCEL for Chemists*; Wiley-VCH: New York, 2001.
(50) Gampp, H.; Maeder, M.; Meyer, C. J.; Zuberbuehler, A. D. *Talanta* **1985**, *32*, 257–264.
(51) Gans, P.; Sabatini, A.; Vacca, A. *Talanta* **1996**, *43*, 1739–1753.
(52) Gans, P., O'Sullivan, B. *VLpH* (see: http://www.hyperquad.co.uk/vlph.htm), unpublished.

Table 1. Complete Proton Dissociation Equilibria for HOPO Ligands and Their Iron(III) Complexes

equilibrium[a]	K or β	log(K or β)[b]	eq.
$N^2(etLH)_2$			
$H_2N^2(etLH)_2^{2+} \leftrightarrows HN^2(etLH)_2^{+} + H^+$	K_{a1}	-3.7 ± 0.1[c]	1−1
$HN^2(etLH)_2^{+} \leftrightarrows HN^2(etL)(etLH) + H^+$	K_{a2}	-6.1 ± 0.1[c]	1−2
$HN^2(etL)(etLH) \leftrightarrows HN^2(etL)_2^{-} + H^+$	K_{a3}	-7.50 ± 0.08[c]	1−3
$HN^2(etL)_2^{-} \leftrightarrows N^2(etL)_2^{2-} + H^+$	K_{a4}	-8.95 ± 0.02[c]	1−4
$2Fe(H_2O)_6^{3+} + 3HN^2(etLH)_2^{+} \leftrightarrows Fe_2(HN^2(etL)_2)_3^{3+} + 6H^+ + 12H_2O$	K_{230}	*d*	1−5
$2Fe(H_2O)_6^{3+} + 3N^2(etL)_2^{2-} \leftrightarrows Fe_2(N^2(etL)_2)^3 + 6H_2O$	β_{230}	*d*	1−6
$2Fe(HN^2(etL)_2)(H_2O)_2^{2+} + HN^2(etLH)_2^{+} \leftrightarrows Fe_2(HN^2(etL)_2)_3^{3+} + 2H^+ + 4H_2O$	K_2	*d*	1−7
$Fe(H_2O)_6^{3+} + N^2(etL)_2^{2-} \leftrightarrows Fe(N^2(etL)_2)(H_2O)_2^{+} + 4H_2O$	β_{110}	21.08 ± 0.01[e]	1−8
$Fe(H_2O)_6^{3+} + HN^2(etLH)_2^{+} \leftrightarrows Fe(HN^2(etL)_2)(H_2O)_2^{2+} + 2H^+ + 4H_2O$	K_{110}	7.5[f]	1−9
$Fe(HN^2(etL)(etLH))(H_2O)_4^{3+} \leftrightarrows Fe(HN_2(etL)_2)(H_2O)_2^{2+} + H^+ + 2H_2O$	K_{aFe}	-0.96 ± 0.09[c]	1−10
$Fe(H_2O)_6^{3+} + N^2(etL)_2^{2-} + H^+ \leftrightarrows Fe(N^2(etL)(etLH))(H_2O)_4^{2+} + 2H_2O$	β_{111}	22.1 ± 0.1[f]	1−11
$Fe(H_2O)_6^{3+} + HN^2(etLH)_2^{+} \leftrightarrows Fe(HN^2(etL)(etLH))(H_2O)_4^{3+} + H^+ + 2H_2O$	K	8.5[f]	1−12
$Fe(H_2O)_6^{3+} + N^2(etL)(etLH)^{-} \leftrightarrows Fe(N^2(etL)(etLH))(H_2O)_4^{2+} + 2H_2O$	β	14.6[f]	1−13
$N^2(prLH)_2$			
$H_2N^2(prLH)_2^{2+} \leftrightarrows HN^2(prLH)_2^{+} + H^+$	K_{a1}	-3.8 ± 0.1[c]	1−14
$HN^2(prLH)_2^{+} \leftrightarrows HN^2(prL)(prLH) + H^+$	K_{a2}	-5.91 ± 0.09[c]	1−15
$HN^2(prL)(prLH) \leftrightarrows HN^2(prL)_2^{-} + H^+$	K_{a3}	-7.94 ± 0.05[c]	1−16
$HN^2(prL)_2^{-} \leftrightarrows N^2(prL)_2^{2-} + H^+$	K_{a4}	-9.21 ± 0.02[c]	1−17
$2Fe(H_2O)_6^{3+} + 3HN^2(prLH)_2^{+} \leftrightarrows Fe_2(HN^2(prL)_2)_3^{3+} + 6H^+$	K_{230}	18.91[f]	1−18
$Fe(HN^3(etL)_3)^{+} \leftrightarrows Fe(N_3(etL)_3) + H^+$	β_{230}	60.46 ± 0.02[e]	1−19
$2Fe(HN^2(prL)_2)(H_2O)_2^{2+} + HN^2(prLH)_2^{+} \leftrightarrows Fe_2(HN^2(prL)_2)_3^{3+} + 2H^+ + 4H_2O$	K_2	5.71[f]	1−20
$Fe(H_2O)_6^{3+} + HN^2(prLH)_2^{+} \leftrightarrows Fe(HN^2(prL)_2)(H_2O)_2^{2+} + 2H^+ + 4H_2O$	K_{110}	6.60[f]	1−21
$Fe(H_2O)_6^{3+} + N^2(prL)_2^{2-} \leftrightarrows Fe(N^2(prL)_2)(H_2O)_2^{+} + 4H_2O$	β_{110}	20.45 ± 0.04[g]	1−22
$Fe(HN^2(prL)(prLH))(H_2O)_4^{3+} \leftrightarrows Fe(HN^2(prL)_2)(H_2O)_2^{2+} + H^+ + 2H_2O$	K_{aFe}	-1.1 ± 0.1[c]	1−23
$Fe(H_2O)_6^{3+} + N^2(prL)_2^{2-} + H^+ \leftrightarrows Fe(N^2(prL)(prLH))(H_2O)_4^{2+} + 2H_2O$	β_{111}	21.5 ± 0.1[f]	1−24
$Fe(H_2O)_6^{3+} + HN^2(prLH)_2^{+} \leftrightarrows Fe(HN^2(prL)(prLH))(H_2O)_4^{3+} + H^+ + 2H_2O$	K	7.65[f]	1−25
$Fe(H_2O)_6^{3+} + N^2(prL)(prLH)^{-} \leftrightarrows Fe(N^2(prL)(prLH))(H_2O)_4^{2+} + 2H_2O$	β	13.56[f]	1−26
$N^3(etLH)_3$			
$H_2N^3(etLH)_3^{2+} \leftrightarrows HN^3(etLH)_3^{+} + H^+$	K_{a1}	-3.79 ± 0.07[c]	1−27
$HN^3(etLH)_3^{+} \leftrightarrows HN^3(etL)(etLH)_2 + H^+$	K_{a2}	-5.7 ± 0.1[c]	1−28
$HN^3(etL)(etLH)_2 \leftrightarrows HN^3(etL)_2(etLH)^{-} + H^+$	K_{a3}	-7.50 ± 0.02[c]	1−29
$HN^3(etL)_2(etLH)^{-} \leftrightarrows HN^3(etL)_3^{2-} + H^+$	K_{a4}	-8.84 ± 0.03[c]	1−30
$HN^3(etL)_3^{2-} \leftrightarrows N^3(etL)_3^{3-} + H^+$	K_{a5}	-10.40 ± 0.04[c]	1−31
$Fe(H_2O)_6^{3+} + N^3(etL)_3^{3-} \leftrightarrows Fe(N^3(etL)_3)H_{1-}^{-} + H^+ + 6H_2O$	β_{11-1}	17.66 ± 0.09[f]	1−32
$Fe(HN^3(etL)_3)^{+} \leftrightarrows Fe(N_3(etL)_3) + H^+$	K_{aFe2}	-9.68 ± 0.08[c]	1−33
$Fe(H_2O)_6^{3+} + N_3(etL)_3^{3-} \leftrightarrows Fe(N^3(etL)_3) + 6H_2O$	β_{110}	27.34 ± 0.04[e]	1−34
$Fe(H_2O)_6^{3+} + HN^3(etLH)_3^{+} \leftrightarrows Fe(HN^3(etL)_3)^{+} + 3H^+ + 6H_2O$	K_1	5.3[g]	1−35
$Fe(H_2O)_6^{3+} + N^3(etL)_3^{3-} + H^+ \leftrightarrows Fe(N^3(etL)_2(etLH))(H_2O)_2^{+}$	β_{111}	30.44 ± 0.08[g]	1−36
$Fe(HN^3(etL)_2(etLH))(H_2O)_2^{2+} \leftrightarrows Fe(HN_3(etL)_3)^{+} + H^+ + 2H_2O$	K_{aFe1}	-3.10 ± 0.07[f]	1−37

Table 1. Continued

equilibrium[a]	K or β	log(K or β)[b]	eq.
$Fe(H_2O)_6^{3+} + N^3(etL)_2(etLH)^{2-} \leftrightarrows Fe(N^3(etL)_2(etLH))(H_2O)_2^{+} + 4H_2O$	β_{tet}	21.58[f]	1−38
$Fe(H_2O)_6^{3+} + HN^3(etLH)_3^{+} \leftrightarrows Fe(HN^3(etL)_2(etLH))(H_2O)_2^{2+} + 2H^+ + 4H_2O$	K_{111}	8.4[f]	1−39
$Fe(H_2O)_6^{3+} + HN^3(etLH)_3^{+} \leftrightarrows Fe(HN^3(etL)(etLH)_2(H_2O)_4)^{3+} + H^+ + 2H_2O$	K_{112}	*h*	1−40
$Fe(H_2O)_6^{3+} + N^3(etL)(etLH)_2^{-} \leftrightarrows Fe(N^3(etL)(etLH)_2(H_2O)_4)^{2+} + 2H_2O$	β_{bis}	*h*	1−41

[a] Equilibria are shown as proton dissociation reactions except in log β_{111} reactions. Conditional equilibrium constants are given the symbol K and written to show the protonation state of the ligand in solution, including the protonation of the central ring system. The protonation state of the central ring is unimportant to the equilibrium constants determined, as protons will only be released from the HOPO binding moieties of the molecule upon chelation. The overall stability constants, log β, are shown as reactions involving completely deprotonated ligands, regardless of the protonation state of the central ring system, to simplify the representation and calculation of the stability constants. [b] All values were determined at $\mu = 0.10$ M, $T = 25$ °C. Errors shown in Table 1 for equilibrium constant values are derived from a number of sources. For equilibrium constants determined directly or indirectly by competition reaction or spectrophotometric titration, the error represents the standard deviation of the experimentally determined value. For equilibrium constants determined indirectly by linear combination of equilibria and their equilibrium constants, the error was determined by propagation of error of the standard deviations of the summed equilibrium constants. [c] Values and estimated error limits are from direct determination by spectrophotometric titration. Potentiometric titration results are in agreement within the error limits of the titrations. [d] Not determined because of solubility problems, see text. [e] Indirect determination by competition reaction . [f] Indirect determination by linear combination of experimental results. [g] Indirect determination by spectrophotometric titration. [h] Not determined because of lack of protonation constant; see text.

7.1, following eqs 8−10. The spectra measured during this experiment are shown in Supporting Information, Figure S1A.

$$Fe(HN^3(etL)_3)^{+} + HEDTA^{3-} \leftrightarrows FeEDTA^{-} + HN^3(etL)_2(etLH)^{-} \quad (8)$$

$$K_{obs} = \frac{[FeEDTA^{-}][HN^3(etL)_2(etLH)^{-}]}{[Fe(HN^3(etL)_3)^{+}][HEDTA^{3-}]} \quad (9)$$

$$\beta_{110} = \left(\frac{K_{obs}}{\beta_{110,\,EDTA}}\right)^{-1} \quad (10)$$

The stability constant, β_{110} was determined from the measured spectra using the program, SPECFIT.

For the Fe/(N^2(etLH)$_2$) system, a stock solution of Fe(EDTA) was prepared at [Fe^{3+}] = [EDTA] = 1.04×10^{-4} mol dm^{-3} and separated into 2.0 mL aliquots. The competition study was conducted by treating the stock aliquots of Fe(EDTA) complex with concentrations of N_2(etLH)$_2$ ranging from 0 mol equiv to 10 mol equiv of N^2(etLH)$_2$:Fe, as described by eqs 11 and 12, and the solutions were allowed to equilibrate for 24 h before measuring the UV−visible spectra (Supporting Information, Figure S1B)

$$Fe(EDTA)^{-} + H_2N^2(etLH)_2^{2+} + H^+ + 2H_2O \leftrightarrows Fe(H_2N^2(etL)_2)(H_2O)_2^{3+} + H_3EDTA^{-} \quad (11)$$

$$K_{obs} = \frac{[Fe(H_2N^2(etL)_2)(H_2O)_2^{3+}][H_3EDTA^{-}]}{[Fe(EDTA)^{-}][H_2N^2(etLH)_2^{2+}][H^+]} \quad (12)$$

and the final pH (2.3 for all solutions). Using the condition-dependent equilibrium constant (eq 12) and the stability constant of the Fe(EDTA) complex, it was possible to determine the β_{110} (eq 13) for the formation of $Fe(H_2N^2(etL)_2)(H_2O)_2^{3+}$ using the program HYPERQUAD.[51]

$$\beta_{110} = (K_{obs})(\beta_{110,\,EDTA}) \quad (13)$$

Results and Discussion

HOPO Ligand Synthesis. Details of the HOPO ligand synthesis and characterization are given in Supporting Information. The synthesis of an electrophilic 3,2-HOPO imidate salt, **4** (Scheme 1), which can be used for the facile incorporation of the HOPO moiety, was recently disclosed.[45] This reagent reacted with a variety of nucleophiles, including amines, to provide siderophores with a three carbon tether between the nucleophile and the HOPO ring without formation of an amide linkage.[53] Of particular interest is the facile reaction of **4** with secondary amines, which makes it an ideal reagent for the attachment of HOPO binding groups to cyclic polyamines.

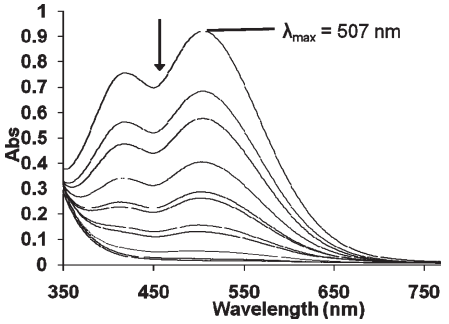

Figure 3. Spectrophotometric measurement of the competition reaction between the $Fe_2(N^2(prL)_2)_3$ complex and EDTA. [Fe^{3+}] = 2.5×10^{-4} mol dm^{-3}, [N^2(prLH)$_2$] = 3.8×10^{-4} mol dm^{-3}, pH = 5.5−7.1, μ = 0.10 (NaCl), [EDTA] = 0−2.5×10^{-3} mol dm^{-3}. Arrow indicates the direction in which the spectrum changes with addition of EDTA.

Scheme 1. Synthesis of Electrophilic HOPO Imidate Salt, **3**

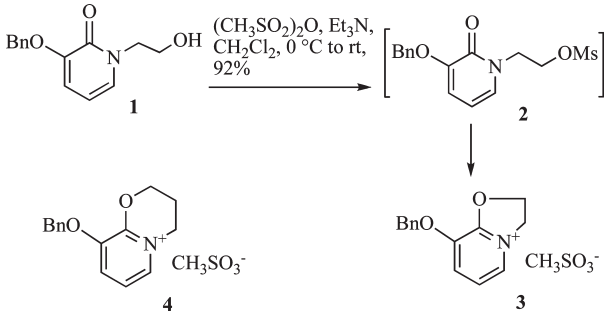

(53) Chittamuru, S.; Lambert, T. N.; Martinez, G.; Jacobs, H. K.; Gopalan, A. S. *Tetrahedron Lett.* **2007**, *48*, 567–571.

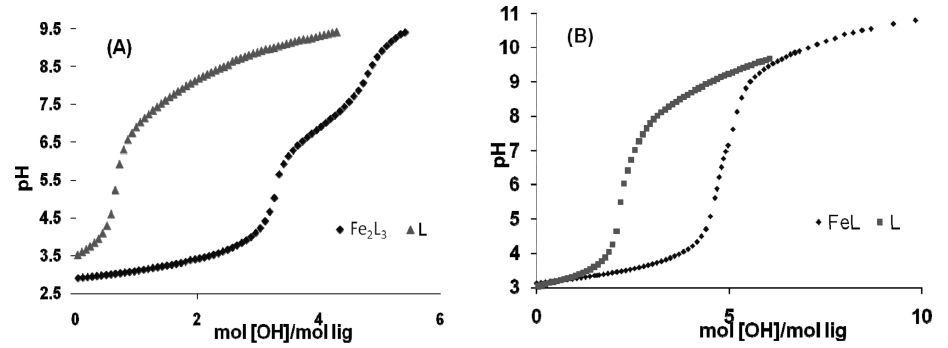

Figure 4. Potentiometric titration of two hydroxypyridinone-Fe^{3+} systems. (A) Fe−N^2(prLH)$_2$ system. [Fe^{3+}] = 4.00×10^{-4} mol dm^{-3}, [N^2(prLH)$_2$] = 6.0×10^{-4} mol dm^{-3}, μ = 0.10 (NaCl). The trace on the left represents the ligand only titration ([N^2(prLH)$_2$] = 6.7×10^{-4} mol dm^{-3}), while the trace on the right represents the Fe-N^2(prLH)$_2$ complex titration. (B) Fe(N^3(etL)$_3$) system. [Fe^{3+}] = 3.98×10^{-4} mol dm^{-3}, [N^3(etLH)$_3$] = 4.0×10^{-4} mol dm^{-3}, μ = 0.10 (NaCl). The trace on the left represents the ligand only titration ([N^3(etLH)$_3$] = 4.0×10^{-4} mol dm^{-3}), while the trace on the right represents the potentiometric titration performed in the presence of 1 equiv of metal.

Scheme 2. Synthesis of Siderophore Mimics N_2(etLH)$_2$ and N_3(etLH)$_3$

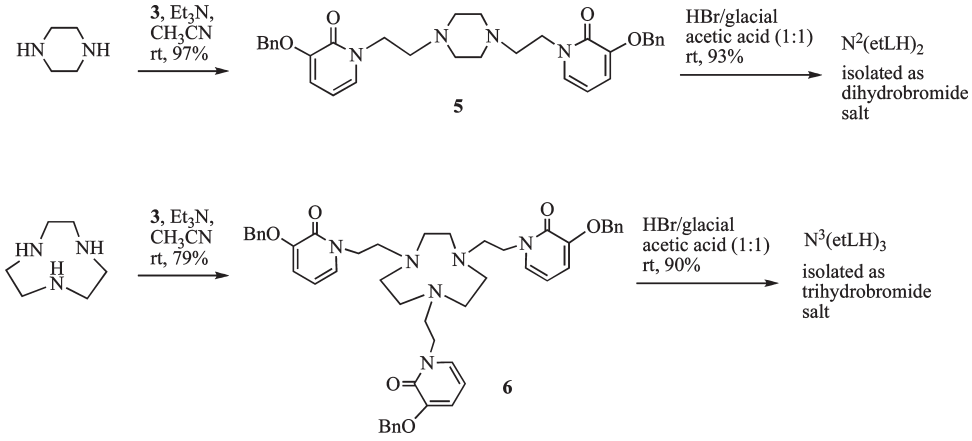

N^2(prLH)$_2$ and other polyHOPO chelators were prepared using **4**.[45]

To prepare HOPO analogues in which the tether between the nucleophile and the HOPO ring is two carbons, the synthesis of HOPO imidate salt **3** was developed (Scheme 1). Preparation of the imidate salt **3** was performed in a manner similar to the method developed for the synthesis of the homologous imidate salt, **4**. Treatment of the known alcohol **1** with methanesulfonic anhydride in dichloromethane in the presence of triethylamine gave the desired bicyclic HOPO imidate salt **3** along with some of the intermediate mesylate **2** (< 10%) as determined by ^{1}H NMR spectral analysis. Complete conversion to the bicyclic salt **3** was achieved by stirring the crude product mixture from the mesylation in chloroform at room temperature. After removal of the solvent, the product was triturated with ethyl acetate. The desired HOPO imidate salt **3** was isolated as a pale white solid in 92% yield in high purity.

The HOPO imidate salt **3** was found to be more reactive than its homologue **4** when reacted with nucleophiles such as amines, alcohols, phenols, thiols, and thiophenols.[54] When piperazine (1 equiv) was treated with the mesylate salt **3** (3 equiv) and triethylamine (4 equiv) in acetonitrile at room temperature the protected HOPO **5** was obtained in 97% yield after chromatographic purification (Scheme 2). Debenzylation with HBr/AcOH (1:1) gave the dihydroxypyridinone N^2(etLH)$_2$ in 93% yield as its dihydrobromide salt. Similarly, treatment of *N*,*N*′,*N*″-1,4,7-triazacyclononane (1 equiv) with the mesylate salt **3** (4.5 equiv) and triethylamine (6 equiv) in acetonitrile at room temperature led to the formation of **6** which underwent debenzylation with HBr/AcOH to give N^3(etLH)$_3$ as a trihydrobromide salt (Scheme 2). It is noteworthy that all three siderophore mimics, N^2(etLH)$_2$, N^2(prLH)$_2$, and N^3(etLH)$_3$ are soluble and stable in water over a wide pH range.

HOPO Ligand Protonation Constants. Protonation constants for N^2(etLH)$_2$, N^2(prLH)$_2$, and N^3(etLH)$_3$ (Figure 2) in aqueous solution were determined by potentiometric and spectrophotometric titration. Potentiometric titration data for the latter two are shown in Figure 4. Representative spectrophotometric titration data for N^2(prLH)$_2$ are shown in Figure 5. The spectral shifts observed in the spectrophotometric titrations correspond to the deprotonation reactions of the hydroxypyridinone moieties of the molecules. As the hydroxypyridinone groups are separate but undergoing identical deprotonation reactions, the spectral shift appeared as a single large shift corresponding to all hydroxypyridinone protonation constants instead of three spectral shifts with separate isosbestic points. In the N^2(prLH)$_2$ titration,

(54) Chittamuru, S.; Martinez, G.; Jacobs, H. K.; Gopalan, A. S., unpublished results.

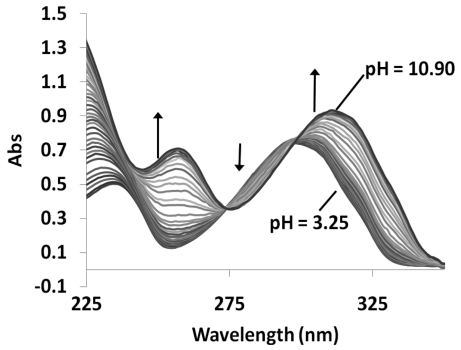

Figure 5. Spectrophotometric titration of the synthetic exocyclic bishydroxypyridinone siderophore $N^2(prLH)_2$ with 0.010 mol dm^{-3} NaOH over the pH range of 3.25 to 10.90. $[N^2(prLH)_2] = 1.0 \times 10^{-5}$ mol dm^{-3}, $\mu = 0.10$ ($NaClO_4$), $T = 25$ °C. Arrows indicate the direction of spectral changes upon addition of base.

isosbestic points were observed at 273 and 298 nm, indicating a transition between two light absorbing species in all recorded spectra (Figure 5). A similar spectral shift was observed in the $N^3(etLH)_3$ titration, with isosbestic points observed at 276 and 300 nm (Supporting Information, Figure S2A). In contrast, the $N^2(etLH)_2$ titration showed similar spectral shifts as in the other two experiments, but only a single isosbestic point was observed at 277 nm (Supporting Information, Figure S2B).

The proton dissociation equilibria are described by eqs 14 and 15 below. The measured deprotonation constants for all three HOPO ligands are shown in Table 1 and Figure 2.

$$LH_n{}^{n-3} \leftrightarrows LH_{n-1}{}^{n-4} + H^+ \quad (14)$$

$$K_{an} = \frac{[LH_{n-1}{}^{n-4}][H^+]}{[LH_n{}^{n-3}]} \quad (15)$$

For the bishydroxypyridinones, $N^2(etLH)_2$ and $N^2(prLH)_2$, four separate deprotonation constants were observed (Figure 2 and Table 1), where pK_{a1} and pK_{a4} correspond to the deprotonation of the ring N atoms and pK_{a2} and pK_{a3} correspond to the hydroxypyridinone donor groups. The deprotonation constants of the ring N atoms are consistent with the observed literature values of [6]ane-N_2 ring systems.[55] The lower pK_a (≈3.7) corresponds to loss of a proton from the doubly protonated ring. This pK_a is greatly depressed because of electrostatic repulsion and steric hindrance.[56] The higher pK_a (9−10) is typical for the deprotonation of the singly protonated [6]ane-N_2 ring. However, it is important to point out that pK_{a1} and pK_{a4} are structurally indistinguishable because of the symmetry of the molecule. After deprotonation of the first polyamine ring proton, the remaining proton will shift to accept electron density from both amine groups. The same is true for pK_{a2} and pK_{a3}, as the deprotonation of one HOPO group will be indistinguishable from the other. The pK_a values that have been assigned to the hydroxypyridinone donor groups are lower than those observed for the 3-hydroxy-2-pyridinone donor group alone, 8.66.[14] It is interesting to note that the average pK_a values observed for the hydroxypyridinone donor groups of $N^2(etLH)_2$ and $N^2(prLH)_2$, 6.80 and 6.92 respectively, are lower than expected and in fact are much closer to the pK_as observed for *retroHOPO*s such as TRENHOPO. For comparison, in the bisHOPO cyclen I the average pK_a of the HOPO donor groups is 8.[57] This may be due to steric or electrostatic considerations. The average pK_a separation for two identical acidic moieties is 0.60 in the absence of any intramolecular interactions, less than the separation observed here (1.4 for $N^2(etLH)_2$ and 2.0 for $N^2(prLH)_2$). This suggests the influence of intramolecular interactions on the pK_a's of the bishydroxypyridinone molecules.[58]

The pK_a values observed for $N^3(etLH)_3$ follow a similar pattern as that observed for the bishydroxypyridinone siderophores (Figure 2 and Table 1). pK_{a1} and pK_{a5} correspond to the central ring system and are significantly separated because of electrostatic repulsion.[59] The third proton on the central ring has a pK_a too low to be observed, also because of steric interactions and electrostatic repulsion from the 2+ doubly protonated ring system. As with the bishydroxypyridinone chelators, it is not possible to make an unambiguous assignment of protonation constants pK_{a2}, pK_{a3}, and pK_{a4} of the $N^3(etLH)_3$ HOPO donor groups. However, it is possible to assign pK_{a1} to the proton of the central ring that is bound to a single amine group and pK_{a5} to the proton that is initially accepting electron density from two amine donors on the central ring. The hydroxypyridinone pK_{a2-4} are 5.7, 7.5, and 8.84 (significant figures are determined based on the standard deviation of the values, as shown in Table 1). The observed pK_a's are separated by more than the predicted separation for three identical acidic moieties, 0.48 log units, implying a contribution from intramolecular interactions.[58] It is interesting that the 3,2-HOPO protonation constants (average pK_a = 7.3) are greater than 2 orders of magnitude more acidic than the 3,2-HOPO protonation constants (average pK_a = 9.5) of TRISPYR (Figure 1).[22] This likely arises because of electrostatic effects resulting from protonation of the central ring system. The protonation constants are also slightly more basic than those observed in TRENHOPO (Figure 1), likely because of the lack of the amide oxygen atoms in the structure of the HOPO donor group arms.[15]

Fe(III)-HOPO Complex Stability and Protonation Constants. General Observations. Iron(III) may be bound by the bidentate HOPO moieties in three modalities as mono, bis, and tris (bidentate, tetradentate, and hexadentate) Fe(III)-HOPO complexes. These complexes exist in solution as a dynamic equilibrium system where mono, bis, and tris coordinated iron(III) complexes interconvert with changing pH because of competition between H^+ and Fe^{3+} for the HOPO oxygen sites (as shown in eqs 16−18, where $HOPO^-$

(55) Khalili, F.; Henni, A.; East, A. L. L. *J. Chem. Eng. Data* **2009**, *54*, 2914–2917.
(56) Luckay, R.; Hancock, R. D.; Cukrowski, I.; Reibenspies, J. H. *Inorg. Chim. Acta* **1996**, *246*, 159–169.
(57) Ambrosi, G.; Formica, M.; Fusi, V.; Giorgi, L.; Guerri, A.; Lucarini, S.; Micheloni, M.; Paoli, P.; Rossi, P.; Zappia, G. *Inorg. Chem.* **2005**, *44*, 3249–3260.
(58) Noszal, B. In *Biocoordination Chemistry: Coordination equilibria in Biologically Active Systems*; Burger, K., Ed.; Ellis Horwood: New York, 1990; pp 18−55.
(59) Geraldes, C. F. G. C.; Alpoim, M. C.; Marques, M. P. M.; Sherry, A. D.; Singh, M. *Inorg. Chem.* **1985**, *24*, 3876–3881.

Table 2. Wavelengths of Maximum Absorbance and Molar Absorptivities for Fe-HOPO Complexes in Aqueous Solution[a]

complex	$N^3(etLH)_3$	$N^2(etLH)_2$	$N^2(prLH)_2$	3-hydroxy-2(1*H*)pyridinone[b]
mono-coordinated	N/A	~600[c]	~600[c]	600
bis-coordinated	546	547	545	548
	(2650 ± 20)	(3580 ± 20)	(3650 ± 50)	(3690)
	413	419	417	415
	(1760 ± 40)	(2400 ± 100)	(2300 ± 200)	(1880)
tris-coordinated	507	508	503	502
	(3820 ± 10)	*d*	(4910 ± 20)	(5160)
	417	418	418	417
	(3320 ± 10)	*d*	(4000 ± 20)	(4080)

[a] Molar absorptivity values (in $dm^3\ mol^{-1}\ cm^{-1}$) from an average of four measurements. [b] Reference 14. [c] Values were measured at high dilution and may be inaccurate. [d] Values were not determined because of low solubility of complex at higher pH.

represents a generic anionic bidentate hydroxypyridinone donor moiety).

$$Fe(H_2O)_6^{3+} + (HOPO)H \leftrightarrows Fe(HOPO)(H_2O)_4^{2+} + H^+ + 2H_2O \quad (16)$$

$$Fe(HOPO)(H_2O)_4^{2+} + (HOPO)H \leftrightarrows Fe(HOPO)_2(H_2O)_2^{+} + H^+ + 2H_2O \quad (17)$$

$$Fe(HOPO)_2(H_2O)_2^{+} + (HOPO)H \leftrightarrows Fe(HOPO)_3 + H^+ + 2H_2O \quad (18)$$

Changes in the Fe(III) inner coordination sphere with pH produce observable changes in the UV−visible spectrum of the solution. The spectral changes observed in this study are in agreement with those previously reported for Fe(III)-3,2-HOPO systems (Table 2).[14]

The determined equilibrium constants for all possible complexation and deprotonation reactions for all three hydroxypyridinone siderophore mimics are shown in Table 1. The values presented were obtained from a combination of direct determination, and indirect determination from competition experiments. The equilibria determined through direct and indirect methods are related through linear combinations of constants determined by other methods and can be used as an internal check for consistency in our equilibrium model.

Bishydroxypyridinone Ligands: $N^2(prLH)_2$ and $N^2(etLH)_2$. Initial complex formation occurs via deprotonation of one hydroxypyridinone donor moiety, which coordinates to the metal center via displacement of two water ligands, as shown in eqs 1−12 and 1−25 in Table 1 (all eqs 1-X designations refer to equilibria listed in Table 1). A gradual increase in pH leads to deprotonation of the second hydroxypyridinone donor group and formation of the tetracoordinate $FeX(H_2O)_2^{+}$ complex (X = $N^2(prLH)_2$ or $N^2(etLH)_2$), shown in eqs 1−10 and 1−23.

The potentiometric titration of the Fe(III)-$N^2(prLH)_2$ system (Figure 4A) showed an initial three-proton buffer region, one proton corresponding to the removal of a single proton from the central ring system and the other two corresponding to the deprotonation of the two HOPO donor groups upon chelation. Figure S3A in the Supporting Information shows the low pH spectrophotometric titration of the Fe(III)-$N^2(prLH)_2$ system. Similar potentiometric and spectrophotmetric data (see Supporting Information, Figure S3B) were obtained for the Fe(III)-$N^2(etLH)_2$ system. The observed changes over the pH range of ~0.2 to 2.5 correspond to conversion of the complex from the bis-coordinate to tetra-coordinate complex, eqs 1−10 and 1−23. Using the spectra measured at low pH, the stability constant of the $FeXH(H_2O)_4^{2+}$ complex (where X = $N^2(etLH)_2$, shown in eq 1−11 or where X = $N^2(prLH)_2$, shown in eq 1−24) was calculated. The value obtained indirectly for the pH independent stability constant of the bishydroxypyridinone complexes, log β_{110}, calculated by spectrophotometric competition titrations (Figure 3) was 20.45 for $Fe(HN^2(prL)_2)(H_2O)_2^{+}$ (eq 1−22) and log β_{110} = 21.08 for $Fe(HN^2(etL)_2)(H_2O)_2^{+}$ (eq 1−8).

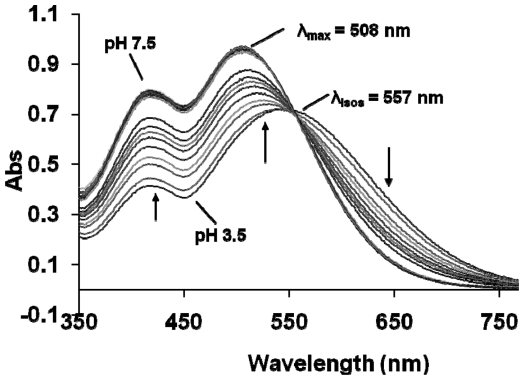

Figure 6. Spectrophotometric titration of the Fe−$N^2(prLH)_2$ system, pH 3.5 to 7.5. $[Fe^{3+}] = 1.99 \times 10^{-4}$ mol dm^{-3}, $[N^2(prLH)_2] = 3.0 \times 10^{-4}$ mol dm^{-3}, $\mu = 0.10$, $T = 25$ °C. Arrows indicate the direction of spectral changes upon addition of base.

At low pH, $N^2(prLH)_2$ and $N^2(etLH)_2$) exhibit similar iron(III) complexation equilibria forming $Fe(HN^2(prL)_2)(H_2O)_2^{+}$ and $Fe(HN^2(etL)_2)(H_2O)_2^{+}$. However, at pH values above 3, their aqueous solution behavior diverges, as discussed below. In the Fe(III)-$N^2(prLH)_2$ system, as the pH increased above where the tetradentate species predominates, a further deprotonation of the free ligand in solution occurred as evidenced by a second buffer region observed in the potentiometric titration (Figure 4A). This second buffer region, from 3 to 5 equiv of base added, corresponds to the formation of the hexacoordinate complex $Fe_2(HN^2(prL)_2)_3^{3+}$, as shown in eq 1−20. Spectrophotometric titration of the Fe(III)-$N^2(prLH)_2$ system over the pH range of 3.5 to 7.5 exhibits a spectral change with an isosbestic point at 557 nm (Figure 6), indicating a single protonation equilibrium.

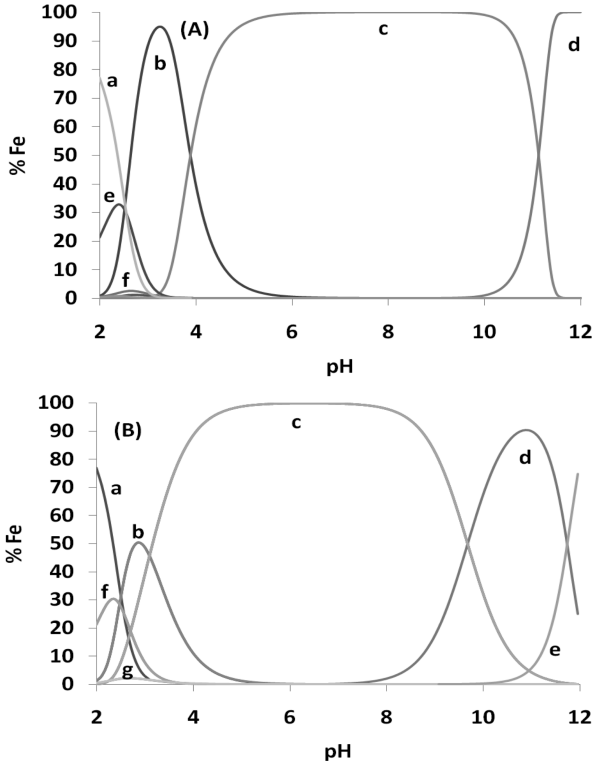

Figure 7. Species distribution diagram for the completely characterized systems of $N^2(prLH)_2$ and $N^3(etLH)_3$ in aqueous solution, showing percent total Fe^{3+} vs pH of solution. Values were calculated from determined stability constants of complexes and hydrolysis constants for Fe^{3+}. $T = 25\,°C$, $\mu = 0.10$. (A) Fe−$N^2(prLH)_2$ system, with $[Fe^{3+}]_{total} = 2.00 \times 10^{-4}$ mol dm^{-3}, and $[N^2(prLH)_2]_{total} = 3.00 \times 10^{-4}$ mol dm^{-3}. a = free Fe^{3+}, b = $Fe(HN^2(prL)_2)(H_2O)_2^{2+}$ complex, c = $Fe_2(HN^2(prL)_2)_3^{3+}$ complex, d = $Fe(OH)_4^-$, e = $Fe(HN^2(prLH)(prL))^{3+}$, and f = $Fe(OH)_2^+$. (B) Fe−$N^3(etLH)_3$ system, $[Fe^{3+}] = 1.00 \times 10^{-4}$ mol dm^{-3}, $[N^3(etLH)_3] = 1.00 \times 10^{-4}$ mol dm^{-3}. a = free Fe^{3+}, b = $Fe(HN^3(etL)_2(etLH))^{2+}$, c = $Fe(HN^3(etL)_3)^+$, d = $Fe(N^3(etL)_3$, e = $Fe(OH)_4^-$, f = $Fe(OH)^{2+}$, and g = $Fe(OH)_2^+$.

The observed shift in λ_{max} is consistent with conversion of the tetracoordinate $Fe(HN^2(prL)_2)(H_2O)_2$ complex to the hexacoordinate $Fe_2(HN^2(prL)_2)_3$ complex (Table 2 and eq 1−20).[14] The equilibrium constant for eq 1−18 is sufficiently high that direct measurement is not possible. Consequently, an indirect stability constant determination by competition with EDTA (see Experimental Section) yielded a log β_{230} value of 60.46 for $N^2(prLH)_2$ (eq 1−19). The species distribution diagram for the Fe(III)-$N^2(prLH)_2$ system (Figure 7A) shows that at the chosen concentrations the Fe(III) is present as a hexacoordinate $Fe_2(HN^2(prL)_2)_3^{3+}$ complex over the pH range of approximately 5 to 10.

Similar behavior is observed in the Fe(III)-$N^2(etLH)_2$ system shown in eqs 1−5 through 1−7; however, the $Fe_2(HN^2(etL)_2)_3$ complex precipitates above pH 3, making it difficult to accurately determine log β_{230}. The complex λ_{max} can be estimated from the remaining absorbance, as shown in Table 2. Comparison to the determined λ_{max} values of the Fe(III)-$N^2(prLH)_2$ complex shows that the Fe(III)-$N^2(etLH)_2$ complex exhibits a similar inner coordination sphere as the $N^2(prLH)_2$ complex at pH 7. Equilibrium constants for eqs 1−10 through 1−13 involving chelation by a single hydroxypyridinone donor group were calculated through EDTA competition experiments (Supporting Information, Figure S1B) and low pH spectrophotometric titrations (Supporting Information, Figure S3). The species distribution diagram for the Fe(III)-$N^2(etLH)_2$ system was not calculated because of the insolubility of the complex at pH > 3.

The tetradentate chelators $N^2(etLH)_2$ and $N^2(prLH)_2$ can reasonably encapsulate a single Fe^{3+} ion or form a bridge between two Fe^{3+} ions. This impacts the possible structures for the 1:1 and 2:3 Fe:X (X = ligand) stoichiometry complexes described here. Specifically, the 1:1 complex can exist in monomeric form ($FeX(H_2O)_2^+$) or as a doubly bridged dimer $(H_2O)_2Fe(\mu\text{-}X)_2Fe(H_2O)_2^{2+}$ (X = $N^2(etLH)_2$ or $N^2(prLH)_2$). The coordinatively saturated 2:3 complex may exist as a singly ((X)Fe(μ-X)Fe(X)) or triply bridged (Fe(μ-X)$_3$Fe) species. To address this question we used ESI-MS to characterize solutions of complexes at the Fe:X ratio and pH conditions where the only species present was FeX as indicated by the speciation plot. The isotopic ratio of ^{56}Fe (91.18% natural abundance) to ^{57}Fe (2.1% natural abundance) is a useful tool to probe the nature of the iron complexes.

There is a peak observed in the Fe(III)-$N^2(etLH)_2$ ESI-MS spectrum that corresponds to the 1:1 complex without coordinated water molecules, $Fe(N^2(etL)_2)^+$ (m/z = 414.1, Supporting Information, Figure S5). The isotopic peaks of the 1:1 complex signal are separated by a whole m/z unit, which implies that the 1:1 complex is present in solution as the monomeric form $Fe(N^2(etL)_2)(H_2O)_2^+$ and not as the ligand-bridged dimer form (see below). A similar isotopic separation is observed in the mass spectrum of the Fe(III)-$N^2(prLH)_2$ 1:1 L:Fe complex system, where the 442.1 m/z peak represents $Fe(N^2(prL)_2)^+$ without coordinated water molecules and exhibits an isotopic

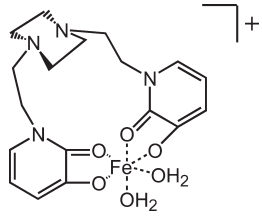

peak separation of 1 m/z unit, also suggesting that the complex is present in aqueous solution as the monomeric $FeX(H_2O)_2^+$ form. If the complexes were found in the ligand bridged dimeric form, $(H_2O)_2Fe(\mu\text{-}X)_2Fe(H_2O)_2^{2+}$, the observed isotopic separation would be 0.5 m/z unit, as the difference in mass-to-charge ratio of the complex arising from the presence of a single ^{57}Fe metal center with the same overall charge of the complex would be 0.5 m/z unit. No peak that corresponds to a possible dimer is observed in the mass spectrum. Peak intensities provide additional evidence for the assignment of the peaks to the FeX^+ complex. Theoretical calculations of the relative peak intensity of the $FeX{+}1^+$ peak for the $Fe(N^2(prL)_2)^+$ complex show that the corresponding isotopic peak should represent 23.5% of the entire peak intensity for all observed isotopes. The observed relative intensity of the $FeX{+}1^+$ peak for the $Fe(N^2(prL)_2)^+$ system was 24.6%, showing very good agreement with the predicted isotopic splitting pattern. A similar calculation for the $Fe(N^2(etL)_2)^+$ system predicted 21.5% of the total peak intensity, and the observed relative intensity of the

$FeX+1^+$ peak was 20%, also showing very good agreement with the predicted isotopic splitting pattern.

On the basis of these observations, we propose that the iron(III) sequestration equilibria for the tetradentate HOPO ligands $N^2(etLH)_2$ and $N^2(prLH)_2$ proceed through the formation of the following structures (R = et or pr).

$$Fe(H_2O)_6{}^{3+} + HN^2(RLH)_2{}^{+} \leftrightarrows Fe(HN^2(RL)_2)(H_2O)_2{}^{2+} + 2H^+ + 4H_2O \quad (19)$$

$$2Fe(HN^2(RL)_2)(H_2O)_2{}^{2+} + HN^2(RLH)_2{}^{+} \leftrightarrows (HN^2(RL)_2)Fe(\mu\text{-}HN^2(RL)_2)Fe(HN^2(RL)_2)^{3+} + 2H^+ \quad (20)$$

Trishydroxypyridinone Ligand: $N^3(etLH)_3$. Initial complex formation of the trishydroxypyridinone ($N^3(etLH)_3$) complex occurs in a similar manner as the bishydroxypyridinone complexes, where addition of iron(III) to the ligand results in displacement of two protons to form the tetracoordinate complex (eq 1−39, Table 1). This complex is formed at a low pH, and the two deprotonation steps are not resolvable, as evidenced by the low pH spectrophotometric and potentiometric titrations. Over the pH range of ~0.2 to 2.5, the spectra that are observed correspond to the formation of the tetracoordinate complex without observing λ_{max} values that correspond to the biscoordinate complex (Supporting Information, Figure S3C). Also, the potentiometric titration (Figure 4B) exhibits an initial 4-proton buffer region that corresponds to the removal of a proton from the central ring, followed by the removal of two protons from hydroxypyridinone donor groups to form the tetracoordinate complex and subsequent removal of a third hydroxypyridinone proton to form the trishydroxypyridinone complex at higher solution pH (eqs 1−39 and 1−37). Spectrophotometric titration of the complex characterized the transition from $Fe(HN^3(etL)_2(etLH))(H_2O)_2{}^{2+}$ to $Fe(HN^3(etL)_3)^+$ over the pH range of ~2.5 to 8, exhibiting a spectral change consistent with the deprotonation of the third donor group to form the hexacoordinate trishydroxypyridinone complex (Supporting Information, Figure S4A). The isosbestic point observed is indicative of a single protonation equilibrium, suggesting deprotonation of a hydroxypyridinone donor group over that pH range (eq 1−37). The measured stability constant for $N^3(etLH)_3$ was found by indirect determination via EDTA competition to be $\log \beta_{110} = 27.34$, eq 1−34.

Between pH 8 and 10.4, another deprotonation event, involving the dissociation of a fourth proton is observed (Supporting Information, Figure S4B) and exhibits an isosbestic point at $\lambda_{max} = 391$ nm. The most likely assignment of this deprotonation event is deprotonation of the central polyamine ring (eq 1−33). This is evidenced by the small changes in absorbance and λ_{max} which suggest a minimal change in the inner coordination sphere of the iron(III). Further, this is consistent with the pK_a, for reaction 1−33, which is ~0.7 log units lower than the pK_a assigned to the less acidic proton dissociation (pK_a = 10.4) of the central ring system of $H_2N^3(etLH)_3{}^{2+}$. Above pH 10.4, the complex began to slowly dissociate, as evidenced by the gradual decrease of the spectral intensity to the baseline.

Table 3. Calculated pFe Values for a Number of Siderophores

ligand	pFe[a]
1-methyl-3-hydroxypyridin-2-one	16.0[b]
Deferiprone	19.4[c]
Deferasirox	23.5[d]
Transferrin	23.6[e]
$N^2(prLH)_2$	24.78[f]
3,4-LI-(Me-3,2-HOPO)	25.5[g]
$N^3(etLH)_3$	26.5[f]
Deferrioxamine B	26.6[h]
TRENHOPO	26.7[i]
HOPObactin	27.4[j]
CP130	27.6[k]
TRISPYR	32.23[l]

[a] pH = 7.4, $[Fe^{3+}] = 1.0 \times 10^{-6}$ mol dm^{-3}, [L] = 1.0×10^{-5} mol dm^{-3}. [b] Ref 63. [c] Ref 64. [d] Ref 65. [e] Ref 66. [f] This work. [g] Ref 16. [h] Ref 67. [i] Ref 40. [j] Ref 15. [k] Determined using equilibrium constants and protonation constants reported in ref 61. [l] Determined using equilibrium constants and protonation constants reported in ref 22.

The species distribution diagram for the Fe(III)-$N^3(etLH)_3$ system as a function of pH is shown in Figure 7B. The plot shows that the Fe(III) is present exclusively as a hexadentate $Fe(HN^3(etL)_3)^+$ complex over the pH range of approximately 5 to 8.

Comparison of Bis- and Tris-HOPO Ligands. A demonstration of the internal consistency of our solution equilibria model shown in Table 1 can be made by comparing the stability constants of complexes of similar denticity. Through linear combination of the protonation constant corresponding to the first hydroxypyridinone moiety of $N^3(etLH)_3$ (eq 1−30) and the $\log \beta_{111}$ (eq 1−36), one can obtain the equilibrium and stability constant shown in eq 1−38. The equilibrium constant for reaction of the doubly deprotonated trishydroxypyridinone ligand $N^3(etLH)_3$ with iron(III) is $\log \beta_{tet} = 21.58$ (eq 1−38), which is very close to the $\log \beta_{110}$ of $N^2(etLH)_2$, 21.08 (eq 1−8). The small increase in the $\log \beta_{tet}$ of $N^3(etLH)_3$ compared to the $\log \beta_{110}$ of $N^2(etLH)_2$ may be due to a chelate effect in $N^3(etLH)_3$ or more favorable steric factors. The similarity of the two values demonstrates that our equilibrium constant determinations are consistent between ligand systems. A similar comparison may be made for the $N^2(prLH)_2$ system, where $\log \beta_{110} = 20.45$ (eq 1−22).

pFe values are a useful criterion to compare iron chelators of different denticities and pK_a's. Table 3 contains pFe values for $N^3(etLH)_3$ and $N^2(prLH)_2$, along with a representative group of comparable chelators listed in ascending order. The high Fe(III) affinity of $N^3(etLH)_3$ and $N^2(prLH)_2$ is reflected by their large pFe values, which are higher than 1-methyl-3-hydroxypyridin-2-one, consistent with their higher denticity and a modest chelate effect. The pFe value observed for $N^3(etLH)_3$ is slightly less than the other tris-HOPO chelators in Table 3, suggesting that the triazacyclononane backbone does not confer significant additional stabilization in the arrangement of the HOPO chelating groups for iron sequestration.

Comparison of the stability of the hexacoordinate complex of $N^3(etLH)_3$ with other HOPO chelators can give an indication of the structural factors that are of

importance in complex formation. Interestingly, comparison of the stability constants would suggest the lack of chelate effect in these macrocyclic hydroxypyridinone siderophore mimics. The measured log β_{110} for $N^3(etLH)_3$ (27.34) can be compared to the log units of complex stability per iron center of the $Fe_2(N^2(etL)_2)_3$ complex($\log \beta_{230}^{1/2} = 30.23$), which would suggest higher stability in the bis-hydroxypyridinone complex. However, using the stability constant β values as the standard of comparison ignores the influence that ligand protonation constants play in aqueous solution complex formation. Therefore, in assessing the effective presence of the chelate effect, it is more appropriate to consider the ligand pFe values. Comparison of the pFe values determined for the $N^3(etLH)_3$ system (26.5) to the $N^2(prLH)_2$ system (24.78) seems to suggest a chelate effect in these exocyclic polyhydroxypyridinone molecules. This may have to do with the structure of the central ring systems as well as different length spacer arms ($N^3(etLH)_3$ has a two carbon chain spacer and $N^2(prLH)_2$ has a three carbon chain spacer), which may contribute to the difference in stability. The determined value of log β_{110} for $N^3(etLH)_3$ also agrees very well with a previously reported value of log $\beta_{110} = 27.6$ for a tripodal tris-hydroxypyridinone siderophore mimic HOPOHL with Fe(III) (Figure 2).[60] It is interesting to note that HOPOHL features amide oxygens in the donor group connector arms. This suggests that the absence of amide bonds in $N^3(etLH)_3$ does not adversely affect the Fe(III) complex stability.

It is additionally important to acknowledge the potential contribution of amide donor groups to the complex stability in some cases. As mentioned previously, amide groups in the spacer arms of the ligand will decrease the aqueous solubility of the molecule. However, at the same time, amide oxygens can contribute to complex stability through the formation of hydrogen bonding networks, resulting in preorganization of the binding cavity. One way of assessing the effect of the amide linkages on complex stability in similar molecules is to compare ligand structures where one features the amide linkages and the other lacks them. Comparison of the pFe values of TRISPYR (pFe = 32.23) and CP130 (pFe = 27.6) (Figure 1), both hexadentate trishydroxypyridinone siderophore mimics, shows more stable chelation by TRISPYR, which lacks the amide functional groups.[22,61] It is possible that in CP130 the amide moieties result in less flexible donor group arms and more unfavorable steric interactions than in TRISPYR. Conversely, the donor arms of TRISPYR do not feature amide functional groups, so the less rigid arms and decreased steric interactions result in more stable complex formation with iron(III). The thermodynamic characterizations of these two chelators were conducted in different solvent systems; however, such a great difference in stability is not likely to be entirely due to solvent effects.

A similar comparison is not necessarily possible for $N^3(etLH)_3$, as a suitable amide containing HOPO model system has not been studied. No binding constants have been reported for the TACN-1-Me-3,2-HOPO, a *retroHOPO* system with amide linkages in the backbone. Structurally, the closest siderophore mimic to $N^3(etLH)_3$ is the *retroHOPO* 3,4-LI-(Me-3,2-HOPO), pFe 25.5, in which the 3,2-HOPO donor groups are linked through amide bonds to an acyclic polyamine platform. Comparison of the pFe values for these chelators suggests that the amide bonds are not critical for iron binding and the overall structure motif/design is more important.

One can also compare $N_3(etLH)_3$ to CP130 to gain insight into the effect of amide bonds on complex stability. The calculated pFe value for CP130 using the reported protonation constants and the equilibrium constant for iron(III) chelation is 28.8, which is significantly higher than that determined for $N^3(etLH)_3$. It is possible that the longer arms of CP130 allows for more stable chelation of iron(III) than does the exocyclic architecture of $N^3(etLH)_3$ because of less steric strain upon binding. The hydroxypyridinone protonation constants of $N^3(etLH)_3$ are slightly more acidic than those of CP130, suggesting that the acidity of the donor groups in $N^3(etLH)_3$ do not provide enough of a thermodynamic advantage to the exocyclic siderophore mimic to overcome the advantage of the less sterically constrained tripodal structure of CP130. A small amount of this difference in stability may also be an artifact of the methods used to calculate pFe values. The protonation constants of the Fe-CP130 complex were not determined, meaning that any protonated form of the complex that would be present in the system are ignored when calculating the complex speciation, which suggest that the pFe values as calculated feature a small error. However, as pFe values are calculated at pH 7.4, it is likely that the protonated forms of the complexes will constitute a relatively minor fraction of total complexed iron at those conditions.

Finally, the pFe values for the chelators prepared in this study make them viable candidates for application as iron overload drugs. Their pFe values are greater than transferrin and superior to the currently approved iron chelation therapy agents Deferasirox and Deferiprone. The pFe value for $N^3(etLH)_3$ is comparable to that of Desferal (desferrioxamine B), the other FDA approved therapeutic for this application. However, there are multiple factors involved in the effectiveness of a chelating agent in iron chelation therapy.[62] Less favorable thermodynamics of iron chelation may be overcome by increasing chelator plasma concentration, and the kinetics of removal of iron from transferrin is also related to the efficiency of a molecule as an iron chelation therapy agent. Previous studies have shown that hydroxypyridinones can rapidly remove iron from transferrin, suggesting that the synthetic HOPO siderophores studied here exhibit iron

(60) Katoh, A.; Kudo, H.; Saito, R. *Heterocycles* **2005**, *66*, 285–297.
(61) Streater, M.; Taylor, P. D.; Hider, R. C.; Porter, J. B. *J. Med. Chem.* **1990**, *33*, 1749–1755.
(62) Turcot, I.; Stintzi, A.; Xu, J.; Raymond, K. N. *J. Biol. Inorg. Chem.* **2000**, *5*, 634–641.
(63) Liu, Z. D.; Hider, R. C. *Coord. Chem. Rev.* **2002**, *232*, 151–171.
(64) Liu, Z. D.; Khodr, H. H.; Liu, D. Y.; Lu, S. L.; Hider, R. C. *J. Med. Chem.* **1999**, *42*, 4814–4823.
(65) Steinhauser, S.; Heinz, U.; Bartholoma, M.; Weyhermuller, T.; Nick, H.; Hegetschweiler, K. *Eur. J. Inorg. Chem.* **2004**, *2004*, 4177–4192.
(66) Martin, R. B.; Savory, J.; Brown, S.; Bertholf, R. L.; Wills, M. R. *Clin. Chem.* **1987**, *33*, 405–407.
(67) Harris, W. R.; Carrano, C. J.; Raymond, K. N. *J. Am. Chem. Soc.* **1979**, *101*, 2722–2727.

binding capabilities in the range that could be of interest in the development of treatments for iron overload.[62]

Conclusions

The investigation of synthetic siderophores can be useful in determining factors of ligand design that lead to increased stability and selectivity in siderophores for Fe(III). This can, in turn, be used for developing new molecules for the treatment of iron overload diseases. One type of binding group that shows promise as a potential candidate for chelation therapy agents is the HOPO donor group. Methodology for the facile synthesis of three synthetic HOPO donor group siderophores has been developed. Further, these synthetic siderophores have shown the ability to form stable complexes with iron at physiological pH, with relative stability comparable to other molecules that are currently in use as iron chelation therapy agents. This could prove useful in the further investigation of new designs for chelation therapy agents.

Acknowledgment. A.L.C. thanks the NSF for financial support (CHE 0809466), the Duke Center for Biomolecular and Tissue Engineering for partial support of J.M.H., and E. M. Tristani and R. D. Hancock for helpful discussions. A.S.G. thanks the National Institutes of Health (PHS Grants S06 GM08136 and 1SC3GM084809-01).

Supporting Information Available: General synthetic methods, procedures and characterization of all compounds; details of spectrophotometric titration methods and selected spectrophotometric titrations; ESI-MS spectra for bishydroxypyridinone-Fe(III) complexes. This material is available free of charge via the Internet at http://pubs.acs.org.